Recognition and Incision of Oxidative Intrastrand Cross-Link Lesions by UvrABC Nuclease†

Chunang Gu,‡ Qibin Zhang,§ Zhengguan Yang,|| Yuesong Wang,§ Yue Zou,|| and Yinsheng Wang*,‡,§

Environmental Toxicology Graduate Program and Department of Chemistry-027, University of California, Riverside, California 92521-0403, and Department of Biochemistry and Molecular Biology, James H. Quillen College of Medicine, East Tennessee State University, Johnson City, Tennessee 37604

Received March 3, 2006; Revised Manuscript Received May 22, 2006

ABSTRACT: Nucleotide excision repair (NER) is a repair pathway that removes a variety of bulky DNA lesions in both prokaryotic and eukaryotic cells. The perturbation of DNA helix structure caused by the oxidative intrastrand lesions could render them good substrates for the NER pathway. Here we employed *Escherichia coli* NER enzymes, i.e., UvrA, UvrB, and UvrC, to examine the incision efficiency of duplex DNA carrying three different oxidative intrastrand cross-link lesions, that is, G[8−5]C, G[8−5m]mC, and G[8−5m]T, and two dithymine photoproducts, namely, the *cis*,*syn*-cyclobutane pyrimidine dimer (T[*c*,*s*]T) and the pyrimidine(6−4)pyrimidone product (T[6−4]T). Our results showed that T[6−4]T was the best substrate for UvrA binding, followed by G[8−5]C, G[8−5m]mC, and G[8−5m]T, and then by T[*c*,*s*]T. The efficiencies of the UvrABC incisions of these lesions were consistent with their UvrA binding affinities: the stronger the binding to UvrA, the higher the rate of incision. In addition, flanking DNA sequences appeared to have little effect on the binding affinity of UvrA for G[8−5]C as AG[8−5]CA was only slightly preferred over CG[8−5]CG. Consistently, these two sequences exhibited almost no difference in incision rates. Furthermore, we investigated the thermal stability of dodecameric duplexes containing G[8−5m]mC or G[8−5m]T, and our results revealed that these two lesions destabilized the duplex, due to an increase in the free energy for duplex formation at 37 °C, by approximately 5.4 and 3.6 kcal/mol, respectively. The destabilizations to the DNA helix caused by those lesions, for the most part, are correlated with the binding affinities of UvrA and incision rates of UvrABC. Taken together, the results from this study suggest that oxidative intrastrand lesions might be substrates for NER enzymes in vivo.

Reactive oxygen species (ROS)[1] can induce damage to various cellular components, including DNA and proteins (*1*, *2*). Other than single-nucleobase lesions, a number of intrastrand cross-link lesions can form from ROS attack (*3*−*15*). In this respect, it was found that intrastrand cross-link lesions G[8−5]C, G[8−5m]T, and G[8−5m]mC (structures shown in Figure 1) can be induced in duplex DNA upon exposure to γ-rays (*8*, *13*, *15*). In addition, our recent study revealed that G[8−5m]T could also be generated from calf thymus DNA upon treatment with Fenton reagent under aerobic conditions (*14*). In mammalian cells, the methylated CpG sites are mutational hotspots and the most frequently observed mutations at these sites are C → T transitions (*16*). In addition, Lee et al. (*17*) reported that, upon treatment with Cu(II), H_2O_2, and ascorbate, a substantial frequency of mCG → TT tandem mutations was observed in NER-deficient XP-A cells but not in repair-proficient cells.

In both prokaryotic and eukaryotic cells, NER is an important pathway for removing bulky base damage or helix-distorting lesions from DNA and thereby maintaining genomic integrity (*18*). Deficiency in NER has been shown to be associated with cancer-prone patients with different complementation groups of xeroderma pigmentosum (XP), Trichothiodystrophy (TTD), and Cockayne's syndrome (*18*, *19*). The *Escherichia coli* UvrABC nuclease system has been employed as a model system for investigating the repair of a variety of bulky DNA lesions. The repair process begins with the DNA damage recognition by the $UvrA_2$−UvrB complex, which binds the damaged sites through at least two steps (*20*), i.e., the recognition of the global duplex distortion by $UvrA_2$ and the subsequent recognition of the specific type of DNA base modifications by UvrB. After the dissociation of $UvrA_2$, the UvrB−DNA complex recruits UvrC to the

† This work was supported by the National Institutes of Health (Grants CA96906 and CA101864 to Yinsheng Wang and CA86927 to Y.Z.) and the University of California Toxic Substances Research and Teaching Program (to C.G.).

* To whom correspondence should be addressed: Department of Chemistry-027, University of California, Riverside, CA 92521-0403. Telephone: (951) 827-2700. Fax: (951) 827-4713. E-mail: yinsheng.wang@ucr.edu.

‡ Environmental Toxicology Graduate Program, University of California.

§ Department of Chemistry-027, University of California.

|| East Tennessee State University.

[1] Abbreviations: NER, nucleotide excision repair; XP, xeroderma pigmentosum; TTD, Trichothiodystrophy; T[*c*,*s*]T, *cis*,*syn*-cyclobutane pyrimidine dimer at the TT site; T[6−4]T, pyrimidine(6−4)pyrimidone product at the TT site; ^{Br}C, 5-bromo-2′-deoxycytidine; ODN, oligodeoxyribonucleotide; T7$^-$, exonuclease-deficient T7 DNA polymerase; HIV-RT, human immunodeficiency virus reverse transcriptase; PAGE, polyacrylamide gel electrophoresis; EMSA, electrophoretic mobility shift assay; T_m, melting temperature; ESI, electrospray ionization; MS/MS, tandem mass spectrometry; ROS, reactive oxygen species.

10.1021/bi060423z CCC: $33.50
Published on Web 08/09/2006

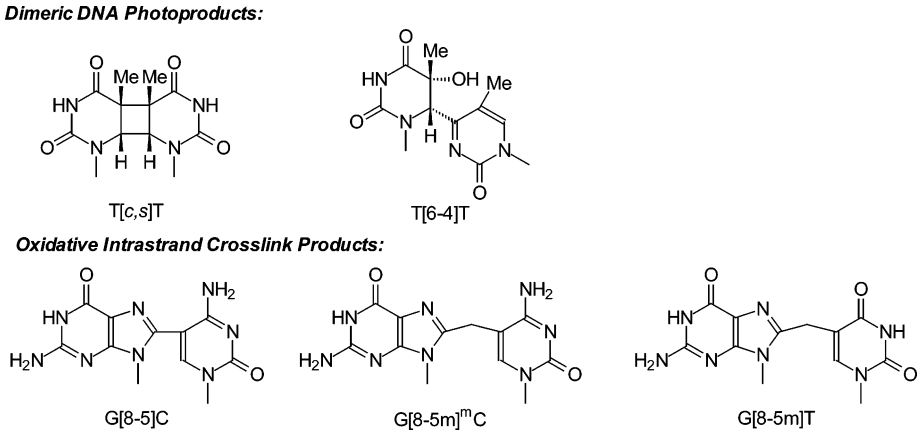

FIGURE 1: Structures of DNA photoproducts and oxidative intrastrand cross-link lesions examined in this study.

damaged site, which triggers the first cleavage at the fourth or fifth phosphodiester bond 3′ to the damage, followed immediately by the 5′ incision at the eighth phosphodiester bond. UvrD helicase then unwinds and removes this 12−13mer damaged DNA strand, and DNA polymerase and ligase seal the gap in the DNA duplex. Although there is no structural homology between the NER proteins in prokaryotes and eukaryotes, they share similar functions of nucleases and overall sequences of the repair process (*18*).

Pyrimidine(6−4)pyrimidone product and its Dewar valence isomer, i.e., T[6−4]T (Figure 1) and T[Dewar]T, are known to be good substrates for the UvrABC nucleases, which are attributed, at least in part, to the large structural distortion to duplex DNA induced by the two lesions (*21*, *22*). In contrast, another major UV photoproduct formed at the TT site, the *cis*,*syn*-cyclobutane pyrimidine dimer (T[*c*,*s*]T, Figure 1), cannot be repaired efficiently by NER (*22*). This latter lesion, however, can be bypassed in an error-free manner by translesion synthesis with polymerase η (*23*, *24*).

Only a few studies that examined the biological effects of oxidative intrastrand lesions have been carried out. In this context, we reported recently that the intrastrand cross-link lesion formed between guanine and cytosine, G[8−5]C (Figure 1), could stall replicative DNA polymerases, i.e., the exonuclease-free (exo$^-$) Klenow fragment of *E. coli* DNA polymerase I, exo$^-$ T7 DNA polymerase, and HIV reverse transcriptase (*15*, *25*). The lesion, however, can be partially bypassed by human (unpublished results) and yeast polymerase η, but incorrect nucleotides were preferentially inserted opposite the guanine portion of the lesion (*15*). In addition, G[8−5m]T has recently been shown to be a poorer substrate for UvrABC enzymes than T[6−4]T and the AAF−dG adduct (26).

Herein, we systematically examined the action of *E. coli* UvrABC enzymes on three oxidative intrastrand cross-link lesions, G[8−5]C, G[8−5m]mC, and G[8−5m]T. For comparison, we also investigated the corresponding recognition and incision of the structurally related T[6−4]T and T[*c*,*s*]T in the same sequence context as the G[8−5]C lesion. Furthermore, we examined the thermodynamic properties of G[8−5m]mC and G[8−5m]T, which, in combination with previous thermodynamic studies of G[8−5]C (*25*), allowed us to correlate the UvrABC incision efficiency with the extent of duplex destabilization caused by different lesions.

MATERIALS AND METHODS

Chemicals and Enzymes. All unmodified oligodeoxyribonucleotides (ODNs) used in this study were purchased from Integrated DNA Technologies (Coralville, IA). [γ-^{32}P]ATP was obtained from Amersham Biosciences Co. (Piscataway, NJ). All other chemicals unless otherwise noted were obtained from Sigma-Aldrich (St. Louis, MO). UvrA, UvrB, and UvrC proteins were purified as reported previously (*26*). The purities of these enzymes were estimated to be better than 95%.

Preparation of ODN Substrates Containing Intrastrand Cross-Link Lesions for in Vitro Repair Studies. The preparation of ODNs containing dimeric thymine photoproducts was described previously (*27*). Briefly, d(GTATTAT) was dissolved in H_2O with an AU_{260} of 0.3 in a quartz tube, degassed by argon bubbling for 30 min, and irradiated with 254 nm light, which was generated by a TLC lamp (UVP Inc., Upland, CA), at room temperature for 30 min. The solution was continuously bubbled with argon during irradiation, and after irradiation, the solution was dried with a Speed-Vac.

The photoproduct-containing ODNs were separated by HPLC on a 4.6 mm × 250 mm Apollo C18 column (5 μm in particle size and 300 Å in pore size, Alltech Associates Inc., Deerfield, IL). Buffer A was 50 mM TEAA (pH 6.5), and buffer B consisted of 50 mM TEAA and acetonitrile (70/30, v/v). The gradient program for the mobile phase was as follows: 0% B at 0 min, 20% B at 5 min, 50% B at 45 min, and 100% B at 50 min. The flow rate was 0.8 mL/min, and a UV detector was set at 260 nm to monitor the effluents. The identities of the photoproducts were confirmed by electrospray ionization tandem mass spectrometry (ESI-MS/MS) measurements (*27*).

The lesion-containing substrate d(GTAG[8−5]CAT) was obtained from the Pyrex-filtered UV irradiation of d(GTAG^{Br}-CAT) (^{Br}C designates a 5-bromo-2′-deoxycytidine) under conditions similar to those described previously (*15*, *28*). The irradiation mixture was separated by HPLC as mentioned above, and a 40 min gradient from 0 to 40% methanol in 50 mM phosphate buffer was used. The dodecameric lesion-bearing substrate d(ATGGCG[8−5]CGCTAT) was obtained from the Pyrex-filtered UV light irradiation of a 5-bromocytosine-containing duplex DNA (*15*, *28*).

To prepare ODNs with G[8−5m]mC and G[8−5m]T, we first synthesized ODNs containing a 5-phenylthiomethyl-2′-deoxycytidine or 5-phenylthiomethyl-2′-deoxyuridine (*11*,

Table 1: TT Photoproduct- and Oxidative Intrastrand Cross-Link Lesion-Containing ODNs Used for UvrA Binding and UvrABC Incision Assays[a]

Name	Sequence
T[*c,s*]T-49bp	5′-AGC TAC CAT GCC TGC AC**G TAT[*c,s*]TAT** GCA ATT CGT AAT CAT GGT CAT AGC T-3′
T[6-4]T-49bp	5′-AGC TAC CAT GCC TGC AC**G TAT[6-4]TAT** GCA ATT CGT AAT CAT GGT CAT AGC T-3′
G[8-5]C-49bp	5′-AGC TAC CAT GCC TGC AC**G TAG[8-5]CAT** GCA ATT CGT AAT CAT GGT CAT AGC T-3′
G[8-5]C-54bp	5′-AGC TAC CAT GCC TGC AC**A TGG CG[8-5]C GCT AT**G CAA TTC GTA ATC ATG GTC ATA GCT-3′
G[8-5m]mC-54bp	5′-AGC TAC CAT GCC TGC AC**A TGG CG[8-5m]mC GCT AT**G CAA TTC GTA ATC ATG GTC ATA GCT-3′
G[8-5m]T-54bp	5′-AGC TAC CAT GCC TGC AC**A TGG CG[8-5m]T GCT AT**G CAA TTC GTA ATC ATG GTC ATA GCT-3′

[a] The lesion-bearing ODNs used for ligation are in bold type.

13). After irradiation with 254 nm light under anaerobic conditions, the mixtures were separated by HPLC. The ODN d(ATGGCG[8−5m]TGCTAT) was purified first with the TEAA buffer system and then with phosphate buffer with the gradient programs described above. The ODN d(ATGGCG[8−5m]mCGCTAT) was purified with the TEAA buffer system.

The lesion-bearing heptameric and dodecameric substrates mentioned above were used to construct 49- and 54mer substrates by enzymatic ligation. In this regard, the lesion-carrying ODNs mentioned above were ligated with a 17mer ODN, d(AGC TAC CAT GCC TGC AC) (the 5′-piece), and a 5′-phosphorylated 25mer ODN, d(GCA ATT CGT AAT CAT GGT CAT AGC T) (the 3′-piece), in the presence of a template (Schemes S1 and S2 of the Supporting Information). The resulting 49- or 54mer lesion-bearing ODNs (sequences given in Table 1) were separated from the ligation reaction mixtures by denaturing PAGE and desalted by ethanol precipitation. The purities of the ligation products were confirmed by denaturing PAGE analysis, and the yields for the ligation reactions are shown in Schemes S1 and S2.

Electrophoretic Mobility Shift Assays (EMSAs). Binding affinities of UvrA for the ODNs were determined by EMSAs. The 49- or 54mer lesion-bearing substrates were labeled at the 5′-end with [γ-^{32}P]ATP and annealed with the corresponding complementary strand. The duplex substrate (1 nM) was then incubated with varying concentrations of UvrA in a 20 μL UvrABC buffer, which contained 50 mM Tris-HCl (pH 7.5), 50 mM KCl, 10 mM $MgCl_2$, 5 mM DTT, and 1 mM ATP, at 37 °C for 15 min. A solution of 80% glycerol (v/v, at 37 °C) was added, and the products were resolved on a 3.5% (1/29) native polyacrylamide gel, which was run at 80 V and room temperature (*26*). Gel band intensities of duplex DNA and the DNA−protein complex were quantified by using a Typhoon 9410 Variable Mode Imager (Amersham Biosciences Co.) and ImageQuant version 5.2 (Amersham Biosciences Co.).

From the EMSA results, the fractions of protein-bound duplex were quantified from the radioactivity in each band (*29*). The dissociation constants (K_d) were obtained by nonlinear curve fitting using Origin version 6.0 (Microcal Software, Northampton, MA) with the following equation:

$$\text{fraction of bound DNA} = \frac{[\text{E}]_{\text{Total}}}{[\text{E}]_{\text{Total}} + K_d}$$

where $[\text{E}]_{\text{Total}}$ is the total concentration of UvrA.

Incision Assays. To determine the incision efficiency of UvrABC on different lesion-bearing substrates, we incubated the duplex ODNs (2 nM) with UvrABC (15 nM UvrA, 250 nM UvrB, and 100 nM UvrC) in the UvrABC buffer at 37 °C for the indicated periods of time. The reactions were terminated by adding 100 mM EDTA (2 μL) and formamide gel loading buffer [80% formamide, 1 mg/mL xylene cyanol, and 1 mg/mL bromophenol blue (12 μL)]. The mixture was loaded onto a 12%, 1/29 cross-linked denaturing polyacrylamide gel containing 8 M urea. The percentage of incision was determined from the radioactivities of gel bands corresponding to the incision product and uncleaved DNA. The incision rates were derived from the slope of the plot where the amounts of incision products were monitored as a function of reaction time. The error limits for incision rate were derived from the fitted parameters as described previously (*30*).

Measurement of Melting Curves and Data Processing. The dodecameric ODNs mentioned above harboring G[8−5m]mC or G[8−5m]T were annealed with another 12mer ODN at a 1/1 ratio to form duplexes, which were employed for melting temperature measurements. The specific nucleotide sequences were 5′-ATGGC**XY**GCTAT-3′ (strand 1) and 3′-TACCG**NM**CGATA-5′ (strand 2), where XY was GmC, GT, G[8−5m]mC, or G[8−5m]T and MN was GC or AC (Table 2).

UV absorbance versus temperature profiles were recorded on a Cary 500 spectrophotometer (Varian Inc., Palo Alto, CA), and the ODNs were dispersed in a 1.2 mL solution containing 250 mM NaCl, 10 mM sodium cacodylate, and 0.1 mM EDTA (pH 7.0) at a total ODN concentration (C_t) of 1.0, 1.8, 3.2, 5.6, or 10 μM. The absorbance was recorded in the reverse and forward directions for a temperature range of 80−10 °C at a rate of 1 °C/min, and the melting temperature (T_m) was obtained by the derivative method. The thermodynamic parameters were obtained from the van't Hoff plot (*31*), where the reciprocal of T_m was plotted against $\ln(C_t/4)$:

$$\frac{1}{T_m} = \left(\frac{R}{\Delta H}\right)\ln\left(\frac{C_t}{4}\right) + \frac{\Delta S}{\Delta H}$$

and

$$\Delta G = \Delta H - T\Delta S$$

where R is the ideal gas constant (1.987 cal mol^{-1} K^{-1}). The error limits for ΔG, ΔH, and ΔS derived from fitted parameters were calculated by using previously described equations (*32*).

Table 2: Thermodynamic Parameters of Duplex Formation in a 250 mM NaCl Solution

Duplex	ΔH (kcal/mol)	ΔS (cal/mol K)	$\Delta G_{37°C}$ (kcal/mol)	$\Delta\Delta G_{37°C}$[a] (kcal/mol)
5′-ATGGCGmCGCTAT-3′ 3′-TACCGC GCGATA-5′	-91.8 ± 4.7	-247 ± 13	-15.4 ± 0.3	
5′-ATGGCG[8-5m]mCGCTAT-3′ 3′-TACCGC GCGATA-5′	-59.6 ± 3.5	-160 ± 10	-9.9 ± 0.1	5.4 ± 0.3
5′-ATGGCGTGCTAT-3′ 3′-TACCGCACGATA-5′	-82.0 ± 2.0	-221 ± 5	-13.5 ± 0.1	
5′-ATGGCG[8-5m]TGCTAT-3′ 3′-TACCGC ACGATA-5′	-76.1 ± 4.6	-213 ± 13	-9.9 ± 0.1	3.6 ± 0.1

[a] $\Delta\Delta G_{37°C} = \Delta G_{37°C}$(lesion-containing duplex) − $\Delta G_{37°C}$(undamaged duplex).

RESULTS

Preparation of ODNs Harboring an Intrastrand Cross-Link Lesion. After the UVC irradiation of d(GTATTAT), four major photoproduct-containing ODNs, d(GTAT[*c*,*s*]-TAT), d(GTAT[6−4]TAT), d(GT[ ]ATTAT), and d(G-TATT[ ]AT), can be clearly separated from each other as well as from the starting material by HPLC (Figure S2 of the Supporting Information). The structure characterizations of these products have been reported previously (*27*).

We recently found that the Pyrex-filtered UV light irradiation of a dodecameric duplex, d(ATGGCG^{Br}CGCTAT)·d(ATAGCGCGCCAT), can induce the formation of an intrastrand cross-link lesion where C8 of guanine and C5 of its adjacent 3′-cytosine are covalently bonded (*15*, *28*). Similarly, the Pyrex-filtered UV light irradiation of the single-stranded d(GTAG^{Br}CAT) can result in the generation of the same lesion where the guanine at the fourth position is covalently bonded to the cytosine at the fifth position. The structure of this lesion was further confirmed by ESI-MS and MS/MS analyses of the lesion-bearing substrate [Figure S3 of the Supporting Information; nomenclature for fragment ions follows that of McLuckey et al. (*33*)].

We prepared the G[8−5m]mC- and G[8−5m]T-containing ODN substrates according to previously published procedures (*8*, *13*). In this respect, we synthesized d(ATGGCGYGC-TAT) (Y represents a 5-phenylthiomethyl-2′-deoxycytidine or 5-phenylthiomethyl-2′-deoxyuridine) by using phosphoramidite chemistry (*13*). The lesion-containing dodecamers d(ATGGCG[8−5m]mCGCTAT) and d(ATGGCG[8−5m]-TGCTAT) were purified from the UVC irradiation mixtures of the mercaptonucleoside-bearing ODNs by HPLC. The molecular masses of the two ODNs mentioned above were measured by ESI-MS as 3672.0 and 3673.2 Da, respectively, which are in accordance with the corresponding calculated average masses of 3672.6 and 3673.6 Da, respectively. Moreover, the site of the cross-link was confirmed by the product ion spectra (MS/MS) of the $[M - 3H]^{3-}$ ions of these ODNs (spectra shown in Figures S4 and S5 of the Supporting Information).

With the above lesion-carrying ODNs, we constructed lesion-bearing 49- and 54mer substrates by enzymatic ligation (see Materials and Methods).

Binding Affinities of UvrA for the Lesion-Bearing ODNs. To improve our understanding on the recognition of these lesions by the *E. coli* NER enzymes, we next employed the electrophoretic mobility shift assays (EMSAs) and examined the binding affinities of these 49- and 54mer substrates for UvrA. As depicted in Figure 2A, UvrA assumes a much stronger binding to the lesion-containing substrates than the control undamaged duplex (Figure 2). We next plotted the percentage of bound fraction against the concentration of UvrA and determined K_d by nonlinear regression analysis (Figures 3 and S6 and Table 3). Consistent with previous findings (*22*), T[*c*,*s*]T was the poorest substrate for UvrA with the largest dissociation constant (91 nM), whereas the substrate exhibiting the strongest binding was T[6−4]T (K_d ∼ 11 nM). The K_d values for the two G[8−5]C-bearing substrates with different flanking bases, on the other hand, were 23 nM for AG[8−5]CA and 29 nM for CG[8−5]CG. Thus, the sequences flanking the lesion had little effect on the binding of G[8−5]C-containing substrates to UvrA.

Our results also revealed that the G[8−5m]mC-containing ODN had a lower binding affinity for UvrA (K_d = 49 nM) than the two G[8−5]C-containing ODNs. On the other hand, the structurally related G[8−5m]T-bearing 54mer ODNs had a dissociation constant of 60 nM, which is the second poorest substrate for UvrA binding among all the lesion-carrying substrates that we investigated.

UvrABC Incisions of the Lesion-Containing ODNs. According to the currently accepted mechanism of the UvrABC system, the first cleavage occurs at the fourth or fifth nucleoside 3′ to the damage, followed by incision at the eighth nucleoside 5′ to the lesion (*34*). We observed 13- and 15mer incision products for 49- and 54mer lesion-containing substrates, respectively (Figure 4A,B). Because all substrates were labeled at the 5′-end, the lengths of the labeled incision products were in keeping with the cleavage mechanism of UvrABC.

The initial incision rates of different substrates can provide insights into the repair efficiencies of UvrABC toward different substrates. To this end, we extracted the initial incision rates from the slope of the line where the amounts of incision products were plotted as a function of reaction time (Figure 5). It turned out that the incision rates, for the most part, are correlated with UvrA binding affinity (Table

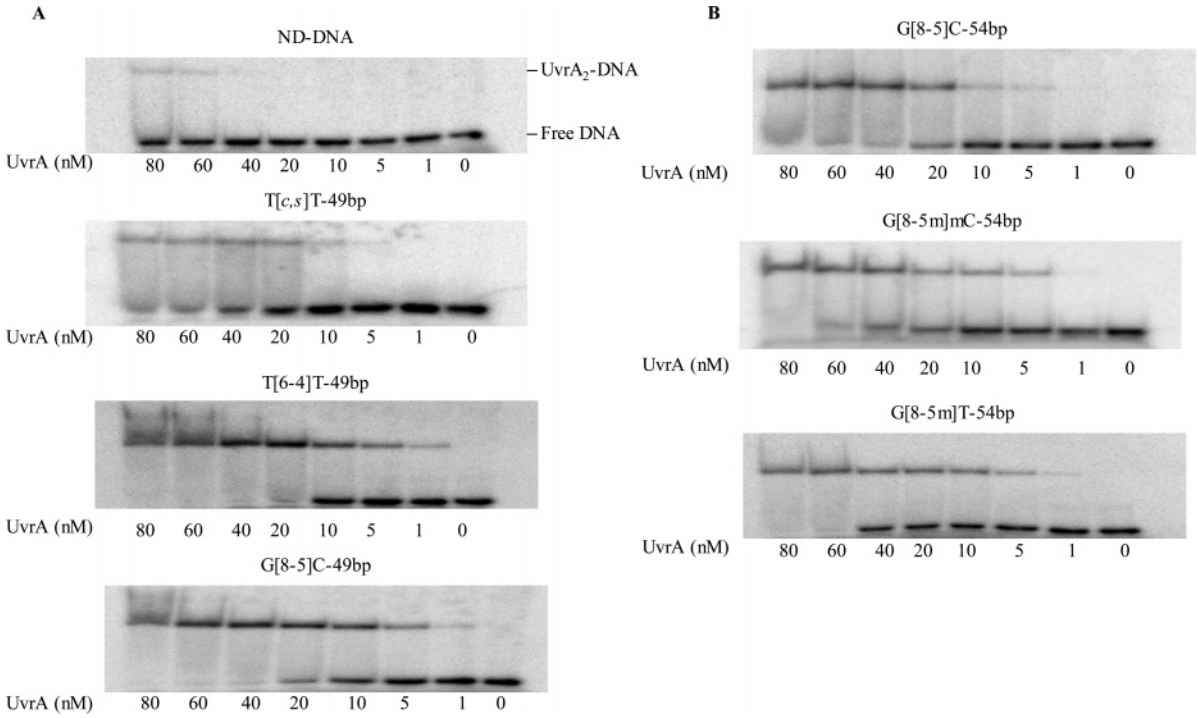

FIGURE 2: Binding of UvrA to (A) undamaged DNA, T[*c*,*s*]T-49bp, T[6−4]T-49bp, and G[8−5]C-49bp and (B) G[8−5]C-54bp, G[8−5m]mC-54bp, and G[8−5m]T-54bp. ODN substrates (1 nM) were incubated with UvrA at the indicated concentrations in UvrABC buffer at 37 °C for 15 min.

Table 3: Equilibrium Dissociation Constants (K_d) for UvrA Binding, Initial Incision Rates of UvrABC, and Free Energy Changes for Duplex Formation

substrate	K_d (nM)	initial incision rate (fmol/min)	$\Delta\Delta G_{37°C}$ (kcal/mol)
T[*c*,*s*]T-49bp	91 ± 9	0.21 ± 0.01	1.5[a]
T[6−4]T-49bp	11 ± 1	0.76 ± 0.04	6.1[a]
G[8−5]C-49bp	23 ± 2	0.47 ± 0.05	
G[8−5]C-54bp	29 ± 3	0.50 ± 0.01	4.0[b]
G[8−5m]mC-54bp	49 ± 4	0.35 ± 0.00	5.4[c]
G[8−5m]T-54bp	60 ± 4	0.30 ± 0.03	3.6[c]

[a] Adopted from ref *21*. [b] Adopted from ref *25*. [c] Based on the thermodynamic data of dodecamers (see Table 2).

3). In line with its highest binding affinity toward UvrA, T[6−4]T-49bp was incised at the highest efficiency by UvrABC. Along this line, T[*c*,*s*]T-49bp exhibited the poorest binding to UvrA, and the initial incision rate was also the lowest, i.e., 0.12 fmol/min. G[8−5]C-containing ODNs had higher incision rates (0.50 fmol/min) than the corresponding ODNs harboring a G[8−5m]mC (0.35 fmol/min) or G[8−5m]T (0.30 fmol/min). In addition, the initial incision rates for AG[8−5]CA-49bp and CG[8−5]CG-54bp were comparable (i.e., 0.47 and 0.50 fmol/min, respectively), which is consistent with what we found for the binding affinities of these two substrates for UvrA. The sequence context, therefore, had little effect on the incision rate of the G[8−5]C-bearing substrates.

Thermodynamic Properties of Lesion-Carrying DNA Duplexes. To understand the biochemical basis of the different binding affinities of UvrA and the different initial incision rates by UvrABC for the five lesions, we next examined the thermodynamic parameters for the G[8−5m]T- and G[8−5m]mC-containing duplexes by melting temperature measurements (Figure 6, details given in Materials and Methods).

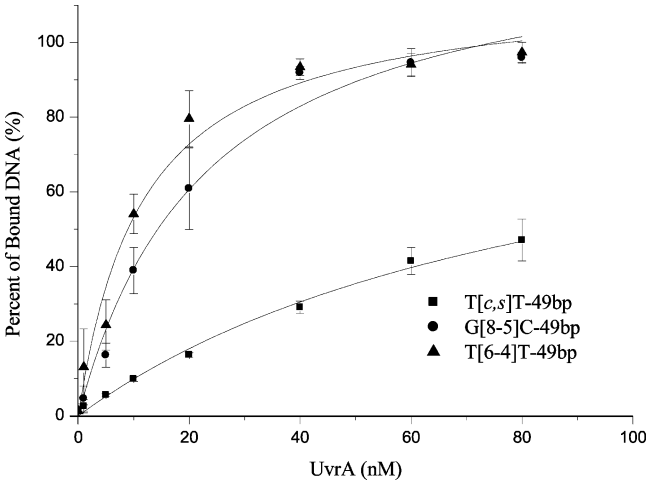

FIGURE 3: Nonlinear regression analysis of the plot of the average percentage of binding (determined from an EMSA with three or more sets of titrations per duplex) vs the concentrations of UvrA for 49mer ODNs containing T[*c*,*s*]T (■), T[6−4]T (▲), and G[8−5]C (●).

In this respect, we used the dodecameric ODNs in the same sequence context as the repair substrates.

It turned out that the presence of G[8−5m]mC destabilized the duplex by 5.4 kcal/mol in free energy at 37 °C, whereas the replacement of GT with G[8−5m]T caused a decrease in the thermal stability of the duplex of 3.6 kcal/mol (Table 2). Our previous study showed that, in the same sequence context, the presence of G[8−5]C can destabilize the duplex by 4.0 kcal/mol (*25*).

DISCUSSION

Recently, several oxidative intrastrand cross-link lesions of DNA have been identified (*3*−*15*). The three lesions employed in this study, that is, G[8−5]C, G[8−5m]mC, and

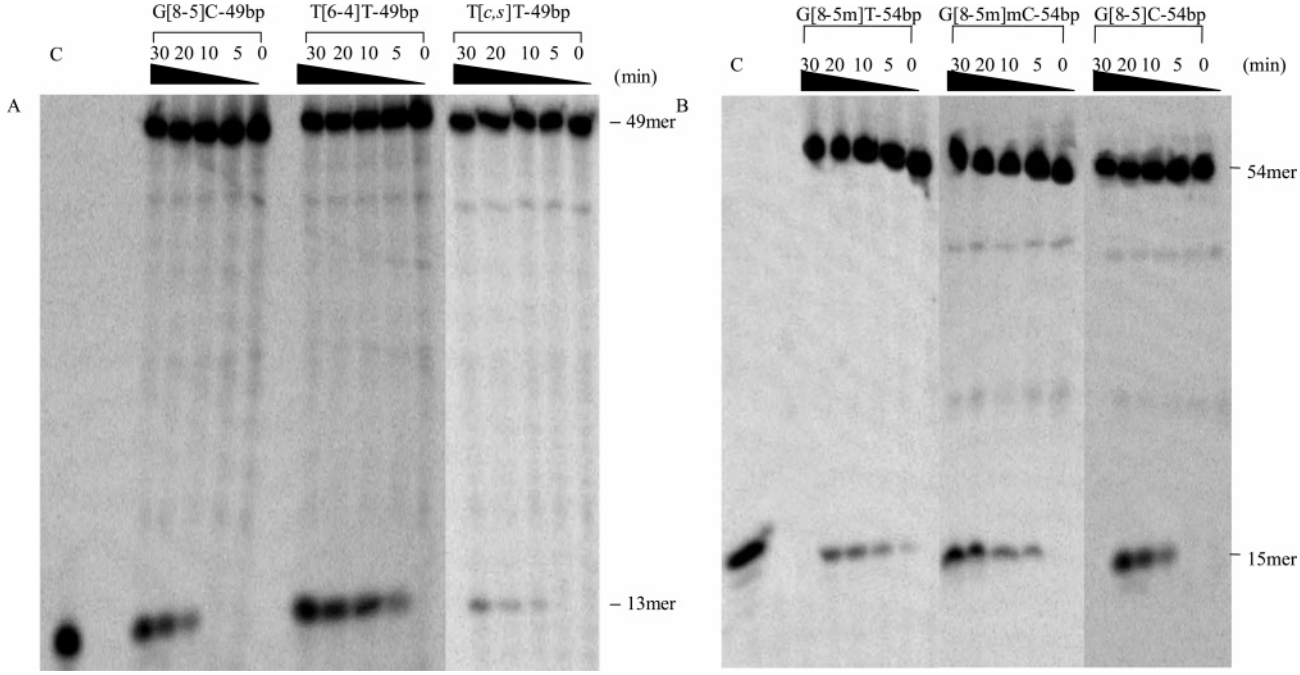

FIGURE 4: UvrABC incision assays of ODNs containing (A) T[*c*,*s*]T-49bp, T[6−4]T-49bp, and G[8−5]C-49bp and (B) G[8−5]C-54bp, G[8−5m]mC-54bp, and G[8−5m]T-54bp. UvrABC was incubated with 2 nM substrates in UvrABC buffer at 37 °C for the indicated periods of time. C indicates control where the known length ODN is loaded. Lanes marked with a C correspond to authentic ODNs with the same sequences as the expected cleavage products: d(AGC TAC CAT GCC T) in panel A and d(AGC TAC CAT GCC TGC) in panel B. The bands observed between the full-length product and 13- or 15mer cleavage product are due to contamination from short ODNs employed for the ligation reaction (integration shows that they constitute a few percent of the full-length product).

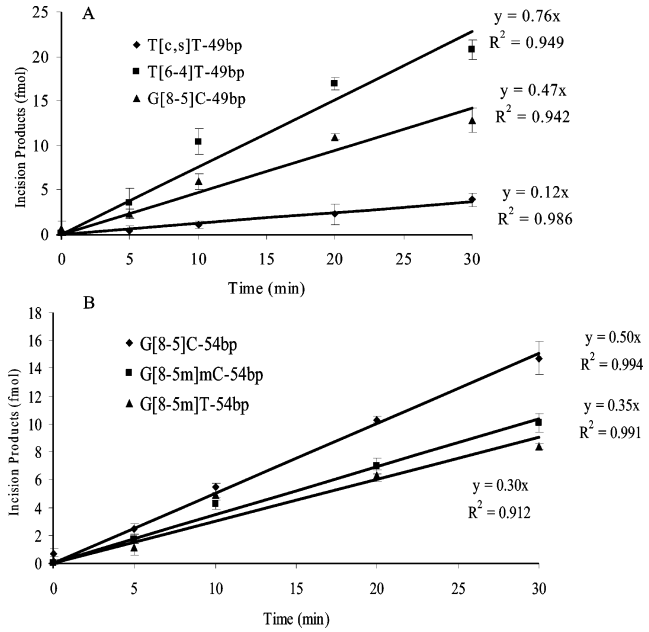

FIGURE 5: Kinetics of UvrABC incisions of DNA substrates: (A) 49mer ODNs containing T[*c*,*s*]T (◆), T[6−4]T (■), and G[8−5]C (▲) and (B) 54mer ODNs containing G[8−5]C (◆), G[8−5m]mC (■), and G[8−5m]T (▲).

G[8−5m]T, could all be induced in duplex DNA upon exposure to γ-ray irradiation (*8*, *13*, *15*). In addition, G[8−5m]T could also form in calf thymus DNA upon treatment with Fenton reagents (*14*). In this context, it is worth noting that G[8−5]C, but not the corresponding C[5−8]G, can be induced in duplex DNA by γ-irradiation (*15*). Likewise, intrastrand cross-link lesions formed between G and T or mC are produced in much higher yields at the GT or GmC site than the corresponding lesions formed at the TG or mCG site (*8*, *13*). Obtaining lesion-bearing ODN substrates constitutes a crucial step in examining the biological implications of these lesions at the molecular level. As we reported previously, a photochemical approach enables us to obtain well-characterized intrastrand cross-link lesion-containing ODNs (*13*, *28*).

To put our studies into the context of previous knowledge about the incision of the two extensively studied UV irradiation-induced thymine dimers, that is, T[*c*,*s*]T and T[6−4]T, by UvrABC enzymes, we also prepared ODN substrates containing these two lesions in the same sequence context as for the G[8−5]C-bearing ODN. Our results with the ODN substrates carrying five different lesions showed that the initial incision rates of UvrABC correlated well with the relative binding affinities of UvrA for the lesion-carrying duplex ODNs. Both the efficiency of UvrABC incision and the affinity of UvrA binding follow the same order: T[6−4]T > G[8−5]C > G[8−5m]mC > G[8−5m]T > T[*c*,*s*]T. This result suggests that these intrastrand cross-link lesions are distinguished primarily in the initial recognition step with UvrA but recognized equally well in the second step by UvrB (*20*).

The thermal stability of the DNA double helix parallels the repair efficiency as long as repair enzymes require a double-stranded substrate (*35*). Thus, the thermal stability measurement may provide some insights into the UvrA recognition mechanism and the following incision reaction by nucleases. Our results showed that this is indeed the case for most substrates examined in this study. T[*c*,*s*]T causes the least destabilization of the DNA helix, which destabilizes duplex DNA by 1.5 kcal/mol of free energy at 37 °C, and has the lowest binding affinity and incision rate among all five substrates (Table 3). T[6−4]T, on the other hand, induces the greatest destabilization of duplex DNA, which

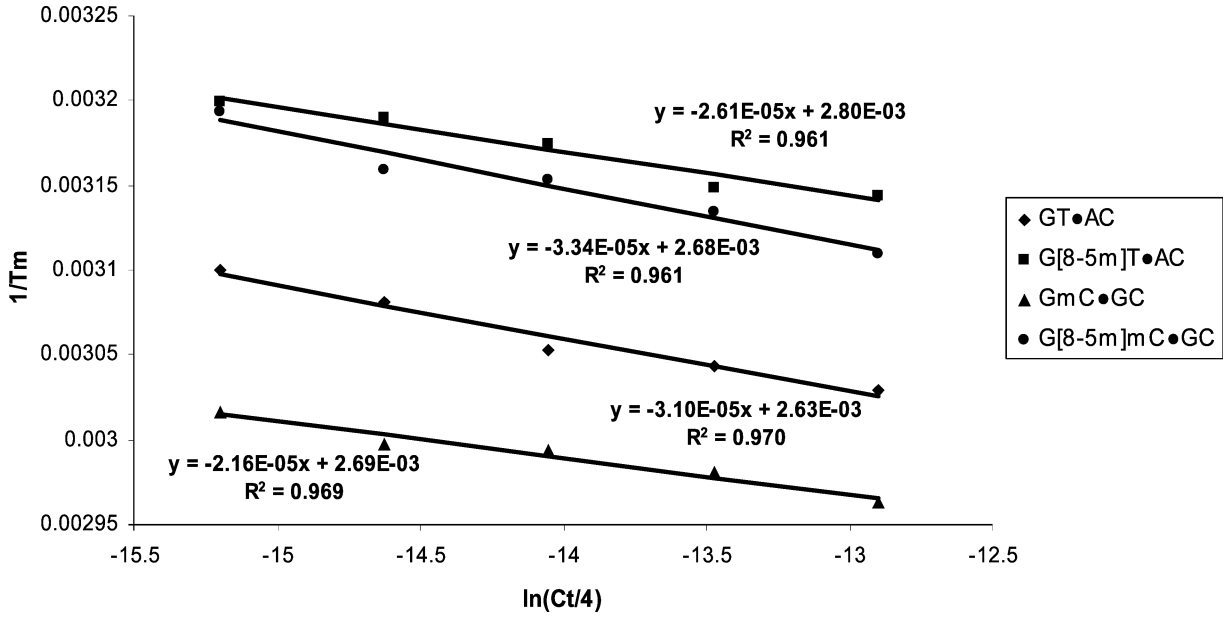

FIGURE 6: Plots of $1/T_m$ vs $\ln(C_t/4)$ for the dodecameric ODN duplexes. The duplex sequence is d(ATGGCXYGCTAT)·d(ATAGCMNGCCAT), where XY·MN represents GmC·GC (▲), G[8−5m]mC·GC (●), GT·AC (◆), or G[8−5m]T·AC (■).

is consistent with the observations that it has the strongest binding affinity for UvrA and can be incised at the highest efficiency (Table 3). These results are also in keeping with previous observations with T[6−4]T (*22*, *26*). When compared with these TT photoproducts, the three oxidative intrastrand cross-link lesions destabilize the duplex more than T[*c*,*s*]T but less than T[6−4]T, which is in line with the fact that the binding affinities and incision rates of oxidative lesions fall between those of the two dithymine photoproducts. In this context, it is worth noting that different dodecameric sequences were employed in determining the thermodynamic parameters for the dithymine photoproducts and intrastrand cross-link lesions (*21*, *25*); different flanking sequences may also contribute partially to the difference in destabilization of DNA duplexes.

The only exception in this group is the G[8−5m]mC-bearing ODN. The presence of the lesion destabilizes the duplex by approximately 5.4 kcal/mol, which is more than that caused by G[8−5]C (4.0 kcal/mol) or G[8−5m]T (3.6 kcal/mol, Table 3). The binding affinity of UvrA and the incision rate for UvrABC toward G[8−5m]mC, however, were similar to those for G[8−5m]T but lower than those for G[8−5]C. The results suggest that other factors may also affect the incision efficiency. The less efficient cleavage by the *E. coli* UvrABC nucleases toward the G[8−5m]mC-bearing substrate prompts us to speculate that this lesion may accumulate more in cells than G[8−5]C. In addition, AG-[8−5]CA-49bp and CG[8−5]CG-54bp, which had different flanking sequences, exhibited a slight difference in UvrA binding and little difference in incision by UvrABC. The dissociation constant for the complex formed between UvrA and CG[8−5]CG-54bp is 29 nM, which is slightly higher than that of the corresponding complex for AG[8−5]CA-49bp (23 nM). This result is consistent with the observations of Zou et al. (*36*), who showed that the flanking bases of A/T cause more destabilization than the flanking bases of C/G and hence can allow the lesion to be recognized more readily by UvrA. However, since the difference in UvrA binding between the two sequences is relatively small, there could be little effect on the incision efficiency at the end.

It is worth noting that free radical can also induce the formation of 8,5′-cyclo-2′-deoxyadenosine (*37*), which is structurally related to oxidative intrastrand cross-link lesions discussed in this paper. Previous studies illustrated that this lesion can also be repaired by NER enzymes (*38*, *39*).

Deficiency in NER results in some severe genetic diseases, such as XP, TTD, and Cockayne's syndrome (*18*, *19*, *40*). Surprisingly, XP patients often have neurological abnormalities due to premature neuronal death (*41*). These neuron losses occur without exposure to UV light, suggesting that these cells are deficient in repairing DNA damage formed by other mutagens (e.g., ROS). Given that neurons consume a large amount of oxygen, oxidative intrastrand cross-link lesions may also accumulate in neuron cells, which may confer neurotoxic effects in XP patients. The repair study of these oxidative intrastrand cross-link lesions by NER enzymes may set a stage for understanding further the pathophysiology of XP patients.

SUPPORTING INFORMATION AVAILABLE

HPLC traces, mass spectrometric characterizations of lesion-containing oligodeoxynucleotides, and UvrA binding curves. This material is available free of charge via the Internet at http://pubs.acs.org.

REFERENCES

1. Lindahl, T. (1999) DNA lesions generated in vivo by reactive oxygen species, their accumulation and repair, *NATO ASI Ser., Ser. A 302*, 251−257.
2. Finkel, T., and Holbrook, N. J. (2000) Oxidants, oxidative stress and the biology of ageing, *Nature 408*, 239−247.
3. Box, H. C., Budzinski, E. E., Dawidzik, J. D., Wallace, J. C., Evans, M. S., and Gobey, J. S. (1996) Radiation-induced formation of a crosslink between base moieties of deoxyguanosine and thymidine in deoxygenated solutions of d(CpGpTpA), *Radiat. Res. 145*, 641−643.
4. Box, H. C., Budzinski, E. E., Dawidzik, J. B., Wallace, J. C., and Iijima, H. (1998) Tandem lesions and other products in X-irradiated DNA oligomers, *Radiat. Res. 149*, 433−439.

5. Box, H. C., Dawidzik, J. B., and Budzinski, E. E. (2001) Free radical-induced double lesions in DNA, *Free Radical Biol. Med. 31*, 856−868.
6. Budzinski, E. E., Dawidzik, J. B., Rajecki, M. J., Wallace, J. C., Schroder, E. A., and Box, H. C. (1997) Isolation and characterization of the products of anoxic irradiation of d(CpGpTpA), *Int. J. Radiat. Biol. 71*, 327−336.
7. Romieu, A., Bellon, S., Gasparutto, D., and Cadet, J. (2000) Synthesis and UV photolysis of oligodeoxynucleotides that contain 5-(phenylthiomethyl)-2′-deoxyuridine: A specific photolabile precursor of 5-(2′-deoxyuridilyl)methyl radical, *Org. Lett. 2*, 1085−1088.
8. Bellon, S., Ravanat, J. L., Gasparutto, D., and Cadet, J. (2002) Cross-linked thymine-purine base tandem lesions: Synthesis, characterization, and measurement in γ-irradiated isolated DNA, *Chem. Res. Toxicol. 15*, 598−606.
9. Liu, Z., Gao, Y., and Wang, Y. (2003) Identification and characterization of a novel crosslink lesion in d(CpC) upon 365 nm-irradiation in the presence of 2-methyl-1,4-naphthoquinone, *Nucleic Acids Res. 31*, 5413−5424.
10. Liu, Z., Gao, Y., Zeng, Y., Fang, F., Chi, D., and Wang, Y. (2004) Isolation and characterization of a novel cross-link lesion in d(CpC) induced by one-electron photooxidation, *Photochem. Photobiol. 80*, 209−215.
11. Zhang, Q., and Wang, Y. (2003) Independent generation of 5-(2′-deoxycytidinyl)methyl radical and the formation of a novel crosslink lesion between 5-methylcytosine and guanine, *J. Am. Chem. Soc. 125*, 12795−12802.
12. Zhang, Q., and Wang, Y. (2004) Independent generation of the 5-hydroxy-5,6-dihydrothymidin-6-yl radical and its reactivity in dinucleoside monophosphates, *J. Am. Chem. Soc. 126*, 13287−13297.
13. Zhang, Q., and Wang, Y. (2005) Generation of 5-(2′-deoxycytidyl)-methyl radical and the formation of intrastrand cross-link lesions in oligodeoxyribonucleotides, *Nucleic Acids Res. 33*, 1593−1603.
14. Hong, H., Cao, H., Wang, Y., and Wang, Y. (2006) Identification and quantification of a guanine-thymine intrastrand cross-link lesion induced by Cu(II)/H_2O_2/ascorbate, *Chem. Res. Toxicol. 19*, 614−621.
15. Gu, C., and Wang, Y. (2004) LC-MS/MS identification and yeast polymerase η bypass of a novel γ-irradiation-induced intrastrand cross-link lesion G[8−5]C, *Biochemistry 43*, 6745−6750.
16. Pfeifer, G. P. (2000) p53 mutational spectra and the role of methylated CpG sequences, *Mutat. Res. 450*, 155−166.
17. Lee, D. H., O'Connor, T. R., and Pfeifer, G. P. (2002) Oxidative DNA damage induced by copper and hydrogen peroxide promotes CG→TT tandem mutations at methylated CpG dinucleotides in nucleotide excision repair-deficient cells, *Nucleic Acids Res. 30*, 3566−3573.
18. Petit, C., and Sancar, A. (1999) Nucleotide excision repair: From *E. coli* to man, *Biochimie 81*, 15−25.
19. Sancar, A. (1996) DNA excision repair, *Annu. Rev. Biochem. 65*, 43−81.
20. Zou, Y., Luo, C., and Geacintov, N. E. (2001) Hierarchy of DNA damage recognition in *Escherichia coli* nucleotide excision repair, *Biochemistry 40*, 2923−2931.
21. Jing, Y., Kao, J. F., and Taylor, J. S. (1998) Thermodynamic and base-pairing studies of matched and mismatched DNA dodecamer duplexes containing cis-syn, (6−4) and Dewar photoproducts of TT, *Nucleic Acids Res. 26*, 3845−3853.
22. Svoboda, D. L., Smith, C. A., Taylor, J. S., and Sancar, A. (1993) Effect of sequence, adduct type, and opposing lesions on the binding and repair of ultraviolet photodamage by DNA photolyase and (A)BC excinuclease, *J. Biol. Chem. 268*, 10694−10700.
23. Johnson, R. E., Prakash, S., and Prakash, L. (1999) Efficient bypass of a thymine-thymine dimer by yeast DNA polymerase, Poleta, *Science 283*, 1001−1004.
24. Masutani, C., Araki, M., Yamada, A., Kusumoto, R., Nogimori, T., Maekawa, T., Iwai, S., and Hanaoka, F. (1999) Xeroderma pigmentosum variant (XP-V) correcting protein from HeLa cells has a thymine dimer bypass DNA polymerase activity, *EMBO J. 18*, 3491−3501.
25. Gu, C., and Wang, Y. (2005) Thermodynamic and in-vitro replication studies of an intrastrand crosslink lesion G[8−5]C, *Biochemistry 44*, 8883−8889.
26. Yang, Z., Colis, L. C., Basu, A. K., and Zou, Y. (2005) Recognition and incision of γ-radiation-induced cross-linked guanine-thymine tandem lesion G[8,5-Me]T by UvrABC nuclease, *Chem. Res. Toxicol. 18*, 1339−1346.
27. Wang, Y., Taylor, J. S., and Gross, M. L. (1999) Differentiation of isomeric photomodified oligodeoxynucleotides by fragmentation of ions produced by matrix-assisted laser desorption ionization and electrospray ionization, *J. Am. Soc. Mass Spectrom. 10*, 329−338.
28. Zeng, Y., and Wang, Y. (2004) Facile formation of an intrastrand cross-link lesion between cytosine and guanine upon Pyrex-filtered UV light irradiation of d(^{Br}CG) and duplex DNA containing 5-bromocytosine, *J. Am. Chem. Soc. 126*, 6552−6553.
29. Valinluck, V., Tsai, H. H., Rogstad, D. K., Burdzy, A., Bird, A., and Sowers, L. C. (2004) Oxidative damage to methyl-CpG sequences inhibits the binding of the methyl-CpG binding domain (MBD) of methyl-CpG binding protein 2 (MeCP2), *Nucleic Acids Res. 32*, 4100−4108.
30. Meyer, S. L. (1975) *Data analysis for scientists and engineers*, Wiley, New York.
31. Breslauer, K. J. (1995) Extracting thermodynamic data from equilibrium melting curves for oligonucleotide order−disorder transitions, *Methods Enzymol. 259*, 221−242.
32. Persmark, M., and Guengerich, F. P. (1994) Spectroscopic and thermodynamic characterization of the interaction of N7-guanyl thioether derivatives of d(TGCTG*CAAG) with potential complements, *Biochemistry 33*, 8662−8672.
33. McLuckey, S. A., Van Berkel, G. J., and Glish, G. L. (1992) Tandem mass spectrometry of small, multiply charged oligonucleotides, *J. Am. Soc. Mass Spectrom. 3*, 60−70.
34. Zou, Y., Liu, T. M., Geacintov, N. E., and Van Houten, B. (1995) Interaction of the UvrABC nuclease system with a DNA duplex containing a single stereoisomer of dG-(+)- or dG-(−)-anti-BPDE, *Biochemistry 34*, 13582−13593.
35. Singer, B., and Hang, B. (2000) Nucleic acid sequence and repair: Role of adduct, neighbor bases and enzyme specificity, *Carcinogenesis 21*, 1071−1078.
36. Zou, Y., Shell, S. M., Utzat, C. D., Luo, C., Yang, Z., Geacintov, N. E., and Basu, A. K. (2003) Effects of DNA adduct structure and sequence context on strand opening of repair intermediates and incision by UvrABC nuclease, *Biochemistry 42*, 12654−12661.
37. Dizdaroglu, M. (1986) Free-radical-induced formation of an 8,5′-cyclo-2′-deoxyguanosine moiety in deoxyribonucleic acid, *Biochem. J. 238*, 247−254.
38. Kuraoka, I., Bender, C., Romieu, A., Cadet, J., Wood, R. D., and Lindahl, T. (2000) Removal of oxygen free-radical-induced 5′,8-purine cyclodeoxynucleosides from DNA by the nucleotide excision-repair pathway in human cells, *Proc. Natl. Acad. Sci. U.S.A. 97*, 3832−3837.
39. Brooks, P. J., Wise, D. S., Berry, D. A., Kosmoski, J. V., Smerdon, M. J., Somers, R. L., Mackie, H., Spoonde, A. Y., Ackerman, E. J., Coleman, K., et al. (2000) The oxidative DNA lesion 8,5′-(S)-cyclo-2′-deoxyadenosine is repaired by the nucleotide excision repair pathway and blocks gene expression in mammalian cells, *J. Biol. Chem. 275*, 22355−22362.
40. Berneburg, M., and Lehmann, A. R. (2001) Xeroderma pigmentosum and related disorders: Defects in DNA repair and transcription, *Adv. Genet. 43*, 71−102.
41. Cleaver, J. E., and Kraemer, K. H. (1989) in *The Metabolic Basis of Inherited Disease* (Scriver, C., Beaudet, A. L., Sly, W. S., and Vale, D., Eds.) Vol. 2, pp 2949−2971, McGraw-Hill, New York.

BI060423Z